U.PORTO

FMUP FACULDADE DE MEDICINA
UNIVERSIDADE DO PORTO

Estimation of Postmortem Interval Based on Cell Death Progression in Biological Fluids

Author: Mónica Cristina Francisco Tomé

Dissertation submitted to the Faculty of Medicine of University of Porto for the Master degree in Forensic Sciences

Supervisor: Prof. Doutor Agostinho Almiro de Almeida
(Faculty of Pharmacy, University of Porto)

Co-supervisors: Prof. Doutor Agostinho José Carvalho dos Santos
(Faculty of Medicine, University of Porto)

Doutora Daniela Sofia Almeida Ribeiro
(Faculty of Pharmacy, University of Porto)

Porto, September 2017

Acknowledgments

My special acknowledgments to:

My supervisor Professor Agostinho Almeida that accepted to work with me and provided me the indispensable help to finish my master degree.

My co-supervisor Professor Agostinho Santos, without him I would not be doing my dissertation, he opened my eyes and I am glad that he did.

My co-supervisor Doctor Daniela Ribeiro that welcomed me with open arms and was always with me.

Doctor Rui Almeida who is a very professional person and who was always ready to help me in whatever it takes!

To Professor Eduarda Fernandes who was always present during the development of this study and was always trying to find solutions to the problems.

To all of my friends, especially to Cátia Pereira, Margarida Pereira, Miguel Pinto and Sofia Salsinha, that provided me the emotional strength to continue to fight and get my motivation.

To my parents and brother, that always listened to me and gave me the emotional support while I was far away from home.

I have to thank also to all of those who were present during this period of my life and never let me give up.

I appreciate the collaboration with the Institute of Legal Medicine and Forensic Sciences, North Branch (Porto).

Abstract

One of the main challenges in forensic medicine is to estimate the postmortem interval (PMI). Several studies regarding postmortem alterations over time in several biological matrices such as vitreous humor and cerebrospinal fluid, among others, have addressed this major question. However, the obtained results from currently available approaches are still unsatisfactory once they have shown no noteworthy changes of the content (e.g. electrolytes, cells, etc.) over time after death (low sensitivity), not granting to estimate the postmortem interval with high accuracy.

The goal of this study is to evaluate the cellular viability, apoptosis state or necrosis state, based on flow cytometry analysis of cells in vitreous humor (VH) and cerebrospinal fluid (CSF) collected from human corpses, in order to correlate it with the postmortem interval. To this qualitative and quantitative evaluation the probes Annexin V labelled with fluorescein and propidium iodide were associated with the trypan blue exclusion test.

In general, CSF presented much higher cellular counts than VH. Therefore, it seems a much more appropriate biological matrix for the intended purpose. Cellular density (cell counts) showed a tendency to increased values with the increasing of PMI only for CSF samples. Also for CSF, a tendency to increased values (from 5.78% to 88.04%) with increasing PMI was observed for viable cells. The other tests parameters (“cells of interest”, “cellular debris”, percentage of cells in apoptosis or necrosis showed conflicting results with each other).

In conclusion, this preliminary study proved that the study of cellular death progression present in VH and CSF can be an important strategy to estimate the PMI. However, more studies are necessary to definitely prove its value.

Keywords: Cell death; cerebrospinal fluid; flow cytometry; postmortem interval; vitreous humor

Table of Contents

Index of Figures

Index of Tables

Index of Appendixes

List of Abbreviations

A5-FITC – Annexin-V labelled with fluorescein isothiocyanate

CSF – Cerebrospinal Fluid

DNA – Deoxyribonucleic Acid

FC – Flow Cytometry

FSC – Forward Scattering

HA – Hyaluronic Acid

NC – Neubauer Chamber

PI – Propidium Iodine

PMI – Postmortem Interval

PS – Phosphatidylserine

RNA – Ribonucleic Acid

SSC – Side Scattering

TB – Trypan Blue

VH – Vitreous Humor

VH-R – Vitreous Humor from right eyeball

VH-L – Vitreous Humor from left eyeball

1. Introduction

1.1. Forensic Medicine

The definition of “Forensic Medicine” has been the subject of some discussion. There has been some differentiation between the terms “Forensic Medicine” and “Legal Medicine”, since for some authors both mean medical knowledge applied to justice, but for others the two terms represent different sciences and roles. According to Beran (2010), Legal Medicine is more comprehensive than Forensic Medicine, focused on solving legal problems in the civil law. Forensic Medicine is the application of biomedical knowledge to the resolution of problems in criminal law. Assuming this perspective, this study is related with the Forensic Medicine concept.

In a criminal investigation of a death there are three major questions to answer: 1) what was the cause of death?; 2) who was involved?; and 3) how long ago did death occur?

The answer to the third question may lead to some clues for the other two, such as the possibility of inclusion/exclusion of suspects at the time of death, exclusion of alibis, among others (Hayman and Oxenham, 2016; Mathur and Agrawal, 2011). Thus, the combination of the subjective evidence, such as witnesses reports, with scientific data can help to clarify many situations (Mathur and Agrawal, 2011).

1.2. Postmortem interval

Postmortem interval (PMI) is defined as the time elapsed since the person died until the body is discovered and analyzed. It is the answer to question 3): “how long ago did death occur?”. As such, one of the main tasks of Forensic Medicine is the determination of this period of time (Lee Goff, 2009; Sachdeva et al., 2011).

After death occurs, several changes begin to happen in the body, not only at a macroscopic level, but also at cellular and molecular levels, being autolysis an example (Hayman and Oxenham, 2016). The evaluation of these changes help in the determination of the time elapsed after the person’s death, i.e., the PMI. Due to physical, physicochemical, metabolic and biochemical changes in the human body there are several phases that can be analyzed in medical-legal autopsies. These phases correspond to a progressive degradation of the body's components, influenced by abiotic

(non-living) factors, such as temperature and humidity, along with biotic factors, such as the activity of microorganisms (Forbes, 2008; Mathur and Agrawal, 2011).

After the stop of heart beating and circulatory activity there is a period that can last up to 100-120 minutes ("supravital period") in which the tissues still respond to stimuli, such as the phenomenon of *algor mortis*, *rigor mortis* and *livor mortis*, which allow the estimation of a PMI (Hayman and Oxenham, 2016; Mathur and Agrawal, 2011):

- ***Algor mortis*** consists in the gradual decrease of the corpse body temperature over time. After death, the body ceases to produce heat and the body temperature tends to be the same as the surrounding environment (Madea and Kernbach-Wighton, 2013; Mathur and Agrawal, 2011). This postmortem phenomenon is used to estimate PMI up to 24 hours after death.

- ***Rigor mortis*** is a physical and chemical phenomenon that consists in the contraction of the body muscles, and begins in the first 2-6h after death, reaching the maximum stiffness between 6h and 12h after death. It can remain up to 72 hours, followed by muscle relaxation until sagging (Gill-King, 1997; Mathur and Agrawal, 2011). This state of contraction is achieved because the body ceases to produce adenosine triphosphate (ATP) and reaches an energy level less than 85%, and consequently the physiologic calcium flux decreases too (Bate-Smith and Bendall, 1947; Madea and Kernbach-Wighton, 2013).

- ***Livor mortis*** consists in the deposition of blood in different parts of the body due to the gravitational force. These zones acquire a characteristic purple coloration. Despite the variability in appearance, it is observed that it can start to occur 15 minutes afterdeath, since it happens as soon as the blood circulation stops, but it becomes more evident 2 hours after. The livors are well developed after 3h-4h and are fixed 8h-12h after death (Clark et al., 1997; Mathur and Agrawal, 2011).

According to Vanezis and Trujillo (1996), *rigor mortis* and *livor mortis,* like *algor mortis,* must be studied together with other parameters in order to estimate PMI more accurately (Madea and Kernbach-Wighton, 2013). The usefulness of this body reactions on the estimation of PMI is valid only on the first hours after death and they are not useful when the body suffered from burns, for example (Mathur and Agrawal, 2011). Other variables can influence the PMI estimation such as climate conditions, body surface, the presence

of antemortem pathologies and the age of the individual, among others. Thus, they represent rather unspecific parameters in the estimation of PMI because they are influenced by many abiotic factors (Hayman and Oxenham, 2016; Kobayashi et al., 2001; Krompecher, 1981; Mathur and Agrawal, 2011).

Another parameter useful to estimate PMI is cadaveric putrefaction, which consists in the degradation of the soft tissues of the corpse by the action of bacteria and endogenous enzymes (autolysis). As a result of the body decomposition, different gases, liquids and salts are produced. Cadaveric putrefaction phases can be divided according to the postmortem time appearance (Mathur and Agrawal, 2011):

1) Chromatic phase: a green spot appears in the right iliac fossa (abdominal spot), with consequent enlargement to the entire abdominal and thoracic wall. At this stage a network of superficial veins in the skin can be observed. This stain is propagated through the corpse and becomes a blue-greenish hue until it becomes a dark spot (Mathur and Agrawal, 2011). This phase appears approximately between 24h and 72h after death, depending on the climate conditions;

2) Emphysematous phase: this is the phase where gases already produced by putrefaction are released and consequently swell the whole body (Mathur and Agrawal, 2011). This phase begins between 2 days to 1 week after death;

3) Tissue reduction phase and liquefaction: at this stage there is softening and disintegration of the tissues, accumulating putrefied fluids (transudate). Epidermal detachment may also occur (Madea and Kernbach-Wighton, 2013; Saukko and Knigth, 2004). This phase occurs 2-3 weeks after death;

4) Skeletonization phase: in this phase the balance between putrefaction and dehydration transforms the transudates into powder (Ubelaker and Zarenko, 2011). This is one of the phases that presents more difficulties in the estimation of PMI because of the preservation of tissues and the consequent delay in decomposition (Hayman and Oxenham, 2016). The time of appearance and duration of this phase depends on the temperature, the condition of the corpse (whether buried or not, for instance) and the presence or absence of decomposition by microorganisms (Madea and Kernbach-Wighton, 2013).

These macroscopic alterations are commonly observed during medical-legal autopsies and are helpful in PMI estimation; however, they are not precise and are difficult to interpret due to the numerous factors that can influence them. As an example, in the different cadaveric putrefaction phases, the autolysis strongly depends on the climatic conditions and consequently it can start in an interval between 48h and 72h after death (Perper, 2006).

The most important factors that increase the rate of decomposition are: temperature (main factor), humidity, the presence of insects and carnivorous animals. On the contrary, submersion in water decreases the rate of decomposition (Prieto et al., 2004).

Besides these parameters, there are also cellular and molecular changes that occur in the cadaver over time that can help in the determination of PMI. (Hayman and Oxenham, 2016) described numerous studies that have been carried out based on these changes:

- Biochemical studies: they are based on the analysis of chemical elements/substances that are released after death and which accumulate in the body. The main studies already performed within this category were based on the evaluation of sodium, potassium, hypoxanthine and oxalic acid levels in different biological specimens, such as VH and synovial fluid. However, the cited studies presented some limitations, as estimation of PMI only 24h after dead, and all of them generally present contradictory results;

- Studies of markers in bone marrow and other organs: studies based on the alteration of cells or proteins over time. The main studies were performed with cells from bone marrow, blood and organs such as heart, and the progression of degradation and morphology alteration over time was evaluated. The studies also presented several limitations, as inaccuracy in the PMI estimated, the fact that the variability of cellular morphology and velocity of changes be too fast to establish a correlation between the studied parameter and the PMI, and the influence of abiotic factors;

- Immunohistochemical studies: studies related to the time of response of certain components to antigens / antibodies in tissue. These studies are based on the biological fluids that contain organic compounds and electrolytes. The main biological matrices used for such studies are VH and CSF. However, the studies presented some flaws such as the process of autolysis to be too fast in cerebrospinal fluid to

study components such as creatinine, insulin, among others and the influence of abiotic factors in the results;

- DNA/RNA studies: studies based of an evaluation of the degradation of nucleic acids after death. The main biological specimens used are the spleen cells and organs such as heart, brain, among others. There are so far no DNA/RNA studies that can be applied in the estimation of PMI in routine forensic practice, due to the high imprecision, the influence of abiotic factors, the high intra-individual variability, the possibility of PMI estimation only after 24 hours after death and the inexistence of correlation between the data and the PMI;

- Entomological studies: those involving the study of insects that colonize the body. This type of studies needs an in-depth knowledge because the correct identification of species and their cycle of reproduction are essential to estimate the PMI, and there is a strong influence of abiotic factors. Besides that, this estimation becomes possible only 3 to 5 days after death because the colonization starts in this period. However, this study is useful for PMIs that are extended to months;

- Studies of bone remains: based on root rings, tendons, ligaments and bones study. Both indirect and direct methods exist. The indirect methods involves palynological and botanical studies, for example the study of root growth rings around the cadaver, but usually results in PMI determinations with high uncertainty. The direct methods consist in the morphological examination of the tendons and ligaments that are still connected at an early stage of skeletonization. These studies are subjective and strongly depend on the investigator experience and knowledge (Hayman and Oxenham, 2016).

1.3. Biological matrices

As previously referred, there are several biological matrices that can be studied in order to estimate the PMI, for instance, blood, bone marrow, different organs, cerebrospinal fluid, vitreous humor and cerebrospinal fluid, among others.

The present study was directed to two biological matrices: vitreous humor (VH) and cerebrospinal fluid (CSF) collected from human corpses. Herein these two matrices will be

described with regard to their anatomical location, cellular composition and main functions.

1.3.1. Vitreous humor

VH is a fluid of gelatinous consistency, representing about 80% of the volume of the eye. It is present between the lens and the retina (**Figure 1**) (Bévalot et al., 2016; Remington, 2011). The total volume of VH in both eyes may reach 4 mL (Angi et al., 2012; Bévalot et al., 2016).

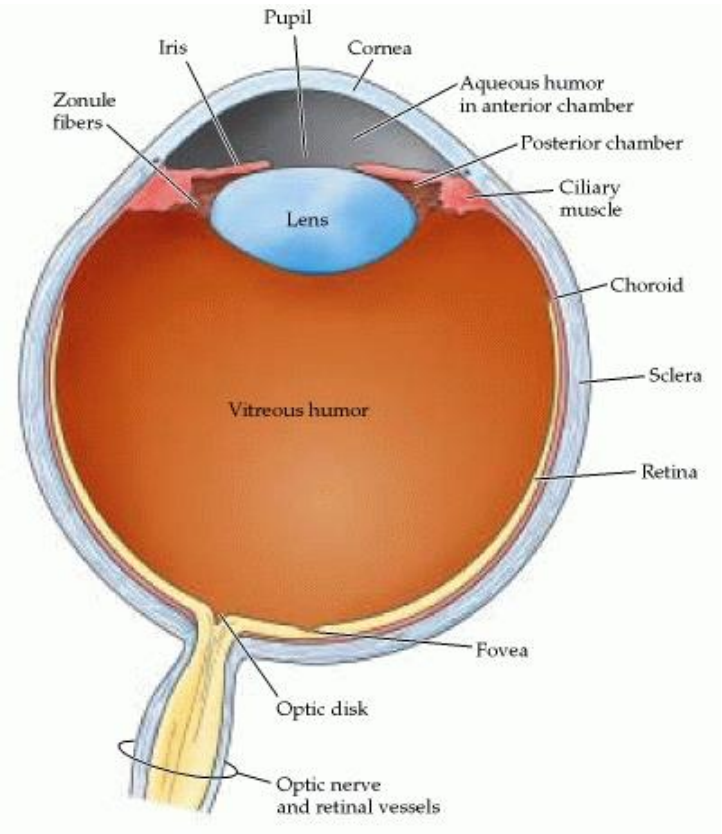

Figure 1 – Anatomic location of VH in the eye (Purves et al., 2001).

Regarding its composition, VH consists essentially of water, dissolved salts, soluble proteins, collagen, hyaluronic acid (HA) and tiny cells – hyalocytes and macrophages (Bévalot et al., 2016; Remington, 2011). Hyalocytes represent the major type of VH cells (Remington, 2011).

The main function of VH is the support and maintenance of the spherical shape of the eye. This fluid functions also as a reservoir of metabolites and thus allows the movement of these metabolites within the eye (Bévalot et al., 2016; Remington, 2011).

1.3.2. Cerebrospinal fluid

CSF is found in the subarachnoid space in the brain (Stratchko et al., 2016). CSF is formed by the choroid plexus of the two lateral ventricles, the 3rd and 4th ventricles. Lateral ventricle fluid converges in the 3rd ventricle through the foramen of Monro and reaches the 4th ventricle via the *aquaeductus cerebri* (Sylvius). The CSF exits from the 4th ventricle through the foramina of Magendie and Luschka to the outer surface of the central nervous system (CNS) (Damkier et al., 2013) (**Figure 2**).

The CSF total volume in the body reaches about 90 to 150 mL, distributed in ventricles (about 20%), in the subarachnoid space (about 15%) and in spinal cord (Puntis et al., 2016; Spector et al., 2015; Stratchko et al., 2016).

CSF is composed by epidermal cells, neutrophils, monocytes and lymphocytes (Bardale, 2009; Johanson et al., 2011; Spector et al., 2015).

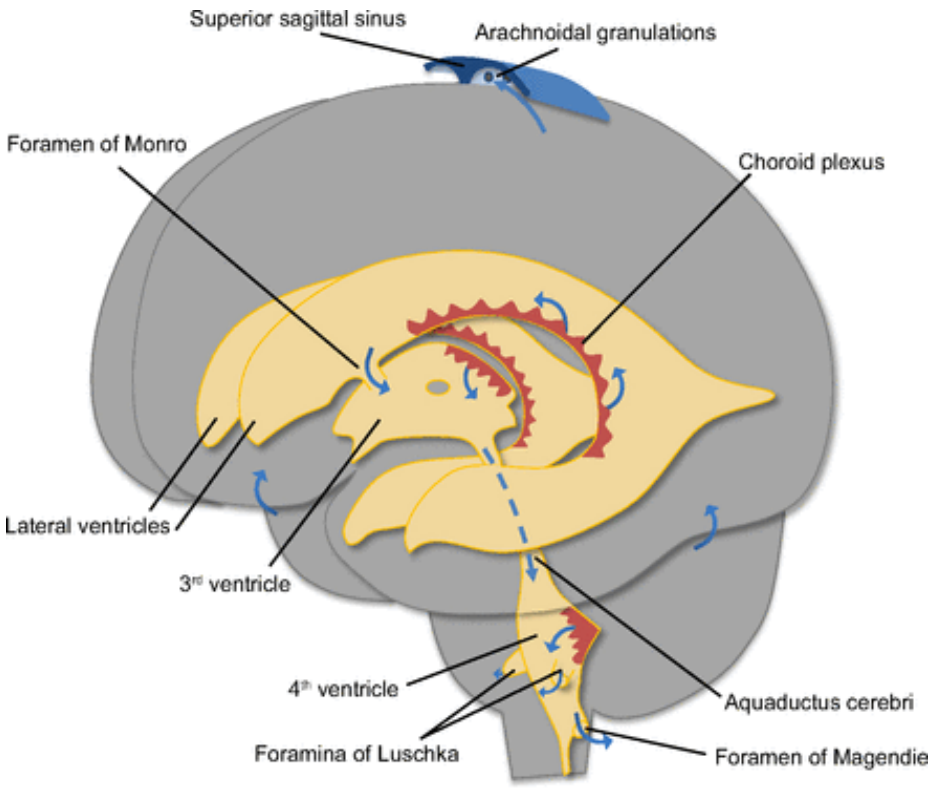

Figure 2 – Organization of the ventricular system of the brain. The brain parenchyma is shown in gray, the ventricles and aquaeductus are in yellow, and the choroid plexus are marked in red (Damkier et al., 2013).

Homeostasis in CNS is achieved because there are physical barriers that protect it: the blood-spinal cord barrier; the CSF barrier and the blood-brain barrier. These barriers are responsible for exchanges between blood and CNS while protecting the parenchyma from toxins, invading pathogens and/or cells (Tenreiro et al., 2016).

1.4. Cell death

Historically, cell death study was focused on one form only: the regulated form – apoptosis. However, over time other forms of cell death have emerged and have been clarified. Currently, cell death can be divided in three different types: apoptosis, autophagic cell death and necrosis (Green, 2017), as seen in **Figure 3**.

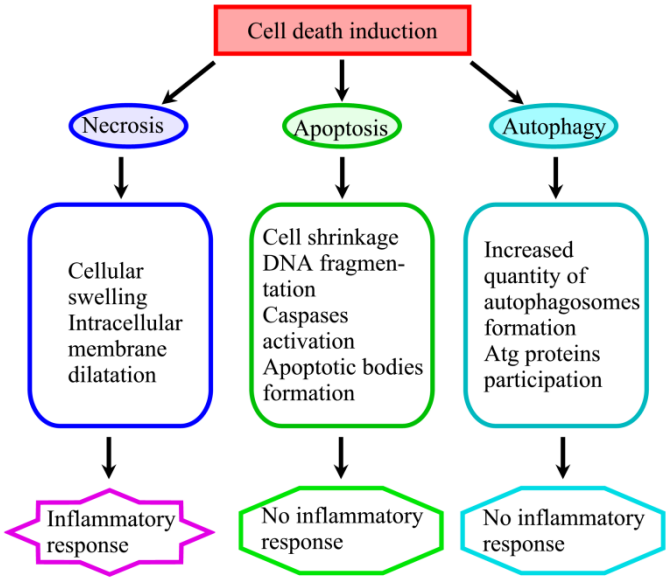

Figure 3 – Characteristics of the necrosis, apoptosis, and autophagic cell death. Each type of cell death has its own morphological and biochemical properties (Escobar-Sánchez et al., 2015).

Apoptosis is an active process that starts when a cell is "marked" for elimination, and this pathway is dependent on effector caspases that are hydrolytic enzymes which have the role of cleaving substrates, consequently activating apoptosis process (Green, 2017).

The pathway in which apoptosis occurs can be divided in extrinsic, here dead receptors are "turned on", and intrinsic or mitochondrial pathway, in which the mitochondrial membrane is permeabilized, releasing proteins that signalize the activation of the caspases (Green, 2017), represented in **Figure 4**.

Cellular alterations include cell wrinkling, organelle damage, coalescence and chromatin displacement to the nucleus margins. The structural alterations are divided in two phases: the first comprises nuclear and cytoplasmic condensation and the breakage of the cell in several conserved fragments that stay next to the plasma membrane, called apoptotic bodies; the second comprises phagocytosis of these bodies, which are drawn from the epithelial surface or are ingested by other cells, where autolysis occurs within the phagosomes and where there is degradation by lysozymes (Kerr et al., 1972).

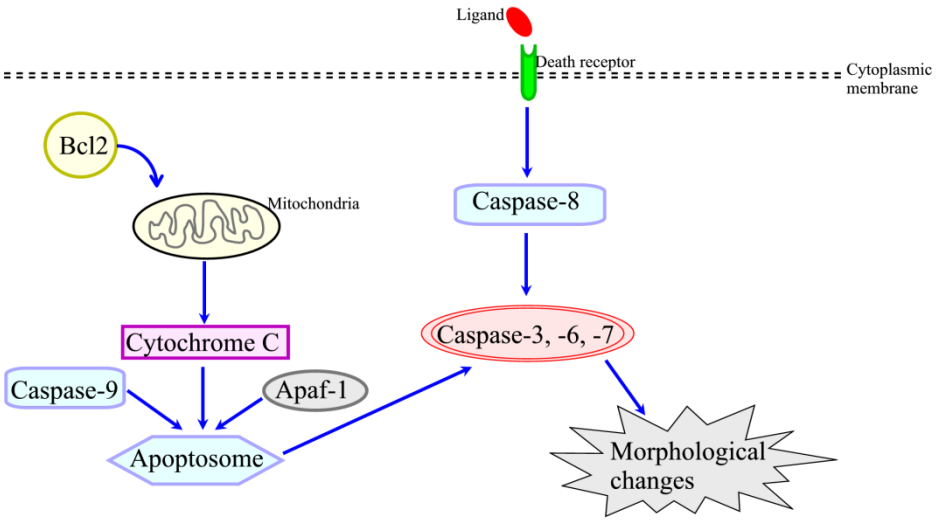

Figure 4 – Intrinsic and extrinsic routes of activation of caspases. Mitochondrial activation involves the cytochrome-C delivering from the mitochondria to form a complex composed by the caspase-9 and the Apaf-1, which in turn will activate the executer caspases -3, -6, or -7. Extrinsic route implies the activation of a death receptor in the cytoplasmic membrane by means of a ligand; this process will activate the initiator caspase-8, which in turn will activate the executer caspase-3, -6, or -7. The activation of the executer caspases provokes the morphological changes related to the apoptotic process (Escobar-Sánchez et al., 2015).

Autophagic cell death can result from either apoptosis or necrosis and is a term applied to invertebrate systems (e.g. *Drosophila*) and to a lesser extent in mammalian cell cultures (Green, 2017).

Necrosis is a term used by pathologists to refer the presence of dead tissues or cells. It represents the changes occurring in the cell after it has already reached equilibrium with the surrounding contents (Majno and Joris, 1995), and involves inflammatory consequences.

Unlike apoptosis, necrosis is seen as a passive and accidental process resulting from environmental disturbances with uncontrolled release of inflammatory cellular contents. It has also been associated with coagulation that is probably the result of an irreversible disturbance of the homeostatic mechanisms of the cell (Fink and Cookson, 2005).

2. Objectives

This study aimed to find a method to estimate the PMI through the analysis of cellular death (apoptosis vs. necrosis) progression of the cells present in two biological matrices with different biochemical composition: vitreous humor (of right and left eyeballs) and cerebrospinal fluid (from subarachnoid space).

To achieve this goal, this work was divided in two steps:

a) Firstly, cell death evaluation in NC with a vital dye was performed and the FC protocol was optimized;

b) Secondly, with all FC parameters duly optimized, the protocol was applied to a set of VH and CSF samples collected from human corpses at different times ranging from 1h30min to approximately 110h after death in order to look for an eventual correlation between PMI and cell death.

3. Materials and Methods

3.1. Reagents

The A5-FITC Apoptosis Detection Kit (cat no. 11858777001) and the Trypan blue 0.4% solution (cat no. 23850) were purchased from Sigma-Aldrich (St. Louis, USA).

3.2. Samples

Samples were collected in compliance with protocol standards of the National Institute of Legal Medicine and Forensic Sciences (INMLCF) - North Branch (Porto), after completing all legal formalities, including the signature of a Term of Responsibility by the study author (**Appendix 1**)**,** and obtaining the necessary authorizations (**Appendix 2**)**.**

After verification of death, the corpses were transported to INMLCF where they were kept under refrigeration until autopsy. All sample's information is presented in **Table 1**.

Samples of vitreous humor from both right (VH-R) and left (VH-L) eyeballs were collected during autopsy with hypodermic puncture needles of 26G 1" 0.45x25 mm and sterile 5 mL Luer-Lock™ syringes (BD Medical, Switzerland).

In the first phase of the work the VH from right and left eyeballs were separately collected to sterile plastic microtubes. In the second phase of the work, VH from both eyeballs were collected to the same sterile Falcon™ tube (BD Biosciences, USA).

Samples of CSF were collected from subarachnoid space with hypodermic puncture needles of 22G ½" 0.7x40 mm and sterile 5 mL Luer-Lock™ syringes to sterile plastic microtubes.

Samples were immediately placed on ice and transported to the laboratory protected from light.

Table 1 – Summary of the sample's information: sample number, gender, age, last time seen alive (date & hour), death verification and autopsy (date and hour), cause of death and associated pathologies, when known. Source: INMLCF, I.P.

Sample nº	Gender	Age (years)	Last time seen alive (estimation: day | hour)	Death Verification (day | hour)	Autopsy (day | hour)	Cause of death	Associated pathologies
1	M	82	11/06/17 | 22h30	12/06/17 | 01h05	13/06/17 | 12h00	Unk	Cardiac
2	F	22	18/06/17 | 20h00	19/06/17 | 14h05	20/06/17 | 16h30	Found hanged	Unk
3	F	41	18/06/17 | 20h00	19/06/17 | 10h40	20/06/17 | 18h00	Found hanged	Unk
4	M	50	25/06/17 | 00h05	25/06/17 | 00h05	26/06/17 | 11h10	Burned	Unk
5	M	58	30/06/17 | 22h50 *	30/06/17 | 22h50	03/07/17 | 11h00	Liver cirrhosis and consumption of toxic substances; found in CRA	Unk
6	F	82	07/07/17 | 11h10 *	07/07/17 | 11h10	10/07/17 | 11h10	Unk	Unk
7	F	50	30/06/17 | 15h00	30/06/17 | 20h00	03/07/17 | 11h00	Voluntary drug intake	Unk
8	F	46	03/07/17 | 00h45	03/07/17 | 1h45	03/07/17 | 16h30	CRA	Unk
9	M	65	01/07/17 | 16h30	01/07/17 | 17h45	03/07/17 | 15h40	Suicide by hanging	Unk
10	M	79	10/07/17 | 00h20 *	10/07/17 | 00h20	10/07/17 | 15h15	Drug intake and CRA	Unk
11	M	62	12/08/17 | 17h25 *	12/08/17 | 17h25	16/08/17 | 11h00	CRA	Unk
12	M	51	12/08/17 | 22h40 *	12/08/17 | 22h40	16/08/17 | 12h00	CRA	Unk
13	M	66	15/08/17 | 21h00	15/08/17 | 21h35	16/08/17 | 16h00	Unk	Diabetes
14	M	66	14/08/17 | 18h00	14/08/17 | 19h00	16/08/17 | 16h30	Unk	Arterial hypertension
15	M	79	15/08/17 | In the morning,36h before 7h29	16/08/17 | 19h29	17/08/17 | 16h00	Tried suicide before	Unk
16	M	55	17/08/17 | 19h	17/08/17 | 19h00	18/08/17 | 16h00	CRA	Epilepsy / dementia
17	F	79	19/08/17 | 08h47 *	19/08/17 | 08h47	21/08/17 | 11h30	CRA	Knees surgery and respiratory dysfunction

CRA – Cardio-respiratory arrest; F – Female; M – Male; Unk – Unknown; * Death at the hospital (so, time of death verification = real time of death).

Table 1 – Summary of the sample's information (cont.). Source: INMLCF, I.P.

Sample nº	Gender	Age (years)	Last time seen alive (estimation: day | hour)	Death Verification (day | hour)	Autopsy (day | hour)	Cause of death	Associated pathologies
18	F	80	19/08/17 at night (considered at 20h)	20/08/17 | 10h20	21/08/17 | 15h30	Unk	Unk
19	M	43	19/08/17 at night (considered at 20h)	20/08/17 | 10h55	21/08/17 | 15h30	Unk	Psychiatric and alcoholic
20	F	48	20/08/17 | 22h55	20/08/17 | 23h55	21/08/17 | 15h30	Liver cirrhosis and alcoholism	Unk
21	M	85	22/08/17 | 10h06 *	22/08/17 | 10h06	23/08/17 | 11h00	Unk	Arterial hypertension, Obesity, sleep apnoea, auricular fibrillation and hypertensive heart disease
22	M	54	Custody death 22h20	21/08/17 | 22h20	23/08/17 | 11h30	Metastatic neoplasm	Unk
23	F	83	23/08/17 | 10h00	23/08/17 | 11h00	24/08/17 | 10h00	Hepatic neoplasm	Unk
24	M	63	23/08/17 | 09h26	23/08/17 | 16h26	24/08/17 | 15h30	Hanging	Psychiatric
25	F	28	23/08/17 (considered at 12h59 because death occurred at lunch, ca. 3h before)	23/08/17 | 14h59	24/08/17 | 15h30	Hanging	Unk
26	M	68	23/08/17 | 15h10 *	23/08/17 | 15h10	25/08/17 | 9h30	Unk	Psychiatric
27	M	74	24/08/17 | 14h50	24/08/17 | 15h50	25/08/17 | 15h00	Unk	Cardiac
28	M	50	24/08/17 | 17h00	24/08/17 | 17h45	25/08/17 | 15h00	Unk	Psychiatric
29	M	67	28/08/17 | 08h00	28/08/17 | 09h36	29/08/17 | 10h30	Hanging	Unk
30	M	44	28/08/17 | 20h30	29/08/17 | 14h30	29/08/17 | 16h00	Unk	Psychiatric
31	M	77	28/08/17 | End of the day (assumed at 18h)	30/08/17 | 08h40	31/08/17 | 15h20	Unk	Unk

CRA – Cardio-respiratory arrest; F – Female; M – Male; Unk – Unknown; * Death at the hospital (so, time of death verification = real time of death).

3.3. Cell counting with Neubauer chamber

3.3.1. Total cell count

Total cell counting was performed with Neubauer Chamber (hemocytometer) in an optical microscope under the 40x objective. Total cell count included all the viable and nonviable cells counted in 4 big squares (**Figure 5**) of the chamber, each one with a volume of 0,1 µL.

To calculate the cellular density the total cell count were divided by total volume (4 x 0,1 µL), resulting in the following equation:

$$Cellular\ Density\ (U/ml) = \frac{(Nº\ of\ cell\ count/4)\ x\ 2\ (dilution\ factor)}{10000}$$

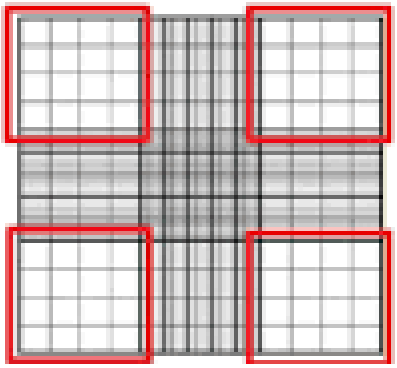

Figure 5 – Counting grid of NC and four of the total nine squares marked in red (Ansari et al., 2013).

3.3.2. Trypan Blue exclusion assay

3.3.2.1. Basis of the method

The dye exclusion test is based on the assumption that viable cells have an intact membrane and consequently dyes cannot pass through it (Strober, 2001). Trypan blue (TB) is a vital stain that gives a blue color to nonviable cells when observed under a microscope, while viable cells appear unstained because nonviable cells does not have the intact membrane and consequently, they are not able to control the entry of macromolecule, letting trypan blue to pass through the cell (Stoddart, 2011).

3.3.2.2. Experimental procedure

Cell viability was determined by the TB exclusion assay. Briefly, 20 µL of sample (VH-R, VH-L and CSF) were mixed 1:1 with trypan blue 0.4% in a microtube and gently mixed. Then, 20 µL of the mixture were loaded into the hemocytometer chamber and the cells observed and counted in an optical microscope under the 40x objective, according to the manual counting procedure described by Stoddart (2011). This procedure was used for subjects no. 1 to 10 (Table 2).

To calculate the percentage of cellular viability, the number of viable cells was divided by the total number of cells and multiplied by 100.

$$Cellular\ viability\ (\%) = \frac{Nº\ of\ viable\ cell\ count}{Nº\ of\ total\ cell\ count}$$

To calculate the percentage of cellular death, the number of dead cells was divided by the total number of cells count and multiplied by 100.

$$Cellular\ death\ (\%) = \frac{Nº\ of\ dead\ cell\ count}{Nº\ of\ total\ cell\ count}$$

3.4. Flow Cytometry

Flow cytometry (FC) methodology allows to count, examine and classify cells of any type (including non-nucleated) in suspension and, since it allows to evaluate these parameters simultaneously, it is currently designated by parametric flow cytometry. This technique has a five element system: the radiation source, the flow chamber, the optical wavelength filter units, the photomultipliers for sensitive detection and signal processing (allowing the distinguishing of probes colors used to stain cells) and the data processing unit collecting (Brown and Wittwer, 2000; Vermes et al., 2000).

In terms of operation it is based on the source of excitation radiation (in general laser) that will intercept the suspended particle in the chamber and this particle undergoes forward scattering (FSC) and in the lateral direction [side scattering (SSC)]. This frontal dispersion is detected by the photomultipliers and the lateral dispersion is deflected 90° by optical

filters and focused on photomultipliers. Frontal dispersion is related to cell size and lateral dispersion with internal complexity (e.g., granularity).
Probes emit radiation too, which associated with a certain internal complexity (SSC) provides relevant information as the physiological state of the cell, among others (Brown and Wittwer, 2000; Vermes et al., 2000).

3.4.1. A5-FITC and PI binding assay

3.4.1.1. Basis of the method

During the early phase of apoptosis, the intensity of the FSC signal decreases due to cell dehydration, and consequent wrinkling. On the contrary, the SSC signal tends to increase because the dehydrated cell further reflects and refracts the light. In more advanced states of apoptosis the FSC decreases, like SSC, because the cells become smaller, and also the ability to reflect and refract light decreases and there are apoptotic bodies being formed (Hingorani et al., 2011; Wlodkowic et al., 2011).

Regarding the necrosis state, in the initial phase the primary necrotic cells have the same behavior as cells in an advanced phase of apoptosis and apoptotic bodies, and they cannot be distinguished from apoptotic cells only by taking into account these two parameters (FSC and SSC). These parameters give a general idea of the state of the cells present in the sample, but cannot be taken into account as reliable markers. However, by combining these FC parameters with the staining with specific dyes it is possible to identify and distinguish cells apoptosis and necrosis with less margin of error (Hingorani et al., 2011; Wlodkowic et al., 2011).

When attempting to discriminate between apoptosis and necrosis, it is important to know their characteristics and to interpret them in their association with the dyes used in the analysis. In the case of apoptosis, the fact that cells keep intact their plasma membrane until about 4h-6h makes them able to exclude propidium iodide (PI), unlike cells that are in the state of cellular necrosis, which allow the dye to enter and to intersperse with DNA and RNA (Arends et al., 1990; Hingorani et al., 2011).

A feature that distinguishes cells in apoptosis from viable cells is the presence of the phospholipid component phosphatidylserine (PS) exposed on the outer surface of the cell membrane, as opposed to what happens in viable cells, where this component is found

only on the inner surface of the membrane. This translocation of PS to the external surface of the cell membrane is dependent on caspases, according to Fink and Cookson (2005).

A5-FITC allows cells to be stained in apoptosis due to its binding to PS, thus differentiating viable cells from apoptotic cells (**Figure 6**).

PI marks the cells in an advanced state of apoptosis and necrosis, allowing to distinguish apoptotic cells from necrotic cells when associated with A5-FITC, as shown in **Figure 6** (Hingorani et al., 2011).

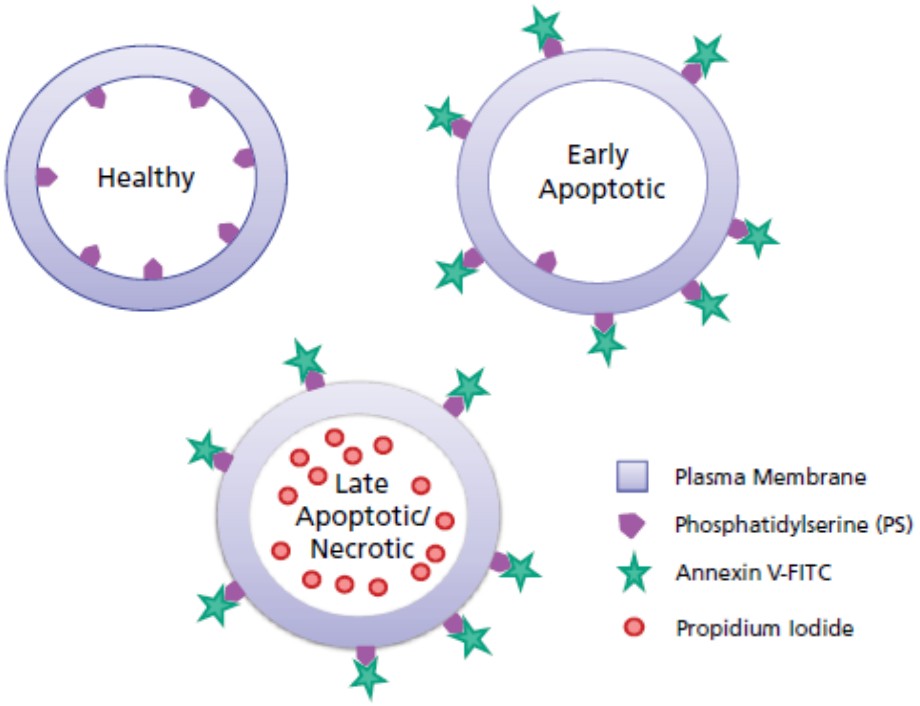

Figure 6 – Diagram showing probes for detection of healthy, apoptotic and necrotic cells (Hingorani et al., 2011).

3.4.1.2. Experimental procedure

A first step of the work consisted in the optimization of the analytical protocol. Samples 1 to 10 (Table 2) were used for this preliminary task.

The samples were centrifuged in 1.5 mL plastic microtubes at 22 °C, at 600 *g* and for 45 min in the case of VH-R and VH-L and for 15 min in the case of CSF. After centrifugation,

the supernatant was aspirated and the pellet was washed with 200 µL of incubation buffer from A5-FITC kit and resuspended. For each sample, the cell suspension was divided by two plastic microtubes (100 µL in each); one tube was labeled as “stained” and the other one as “unstained”. To the “stained” ones, 2 µL of A5-FITC and 2 µL of PI were added. To the “unstained” ones the equivalent volume of incubation buffer of the A5-FITC kit was added. All samples were incubated for 15 min, protected from light. Afterwards, 500 µL of incubation buffer were added to both tubes (“stained” and “unstained”). The content of each tube was then totally transferred to cytometry tubes through filtration by FC filters.

The viability parameters, apoptosis and necrosis, were then analyzed by FC.

Fluorescence signals for each sample were collected using an Accuri™ C6 flow cytometer (BD Biosciences). To restrict the analysis to cells of interest only, a polygon gate (P1) was set according to their light scattering properties (in a forward scatter vs. side scatter plot), thus excluding cell debris. To evaluate the % of cell debris among all samples a polygon gate (P2) was set according to light scattering properties (in a forward vs. side scatter plot) of cell debris.

Fluorescence signals of at least 5,000 and 10,000 cells were acquired for VH-R and VH-L and of at least 25,000, 50,000 and 100,000 cells for CSF, both in logarithmic mode, and the data were analyzed using the Accuri™ C6 flow cytometer software. The green fluorescence due to A5–FITC was followed in channel 1 (FL1) and plotted as a histogram of FL1 staining. Fluorescence due to the PI incorporation was followed in channel 3 (FL3).

Samples marked as “unstained” were analyzed before the “stained” ones, acting as negative controls.

After this previous evaluation of the procedure, the following changes were made on the protocol: a) VH samples from right and left eyeballs were mixed and analyzed together; b) centrifugation was fixed at 600 *g* for 15 min for all the samples; c) fluorescence signals was acquired for 10,000 cells for VH and 100,000 cells for CSF.

b) A5-FITC and PI binding assay

After the establishment of the optimal protocol, samples no. 11 to 31 (n=21) (Table 1) were studied in this second phase of the work.

Cellular density was calculated by the following equation:

$$Cellular\ Density\ (U/mL) = \frac{Nº\ of\ events}{volume\ aspirated\ (ml)}$$

To calculate the final percentage of apoptosis and necrosis, determined based on the percentage of events in the quadrant Q2-LR (lower right) for apoptosis; and on the percentage of events in the quadrant Q2-UR (upper right) for necrosis, of the FL3 (PI staining) x FL1 (A5–FITC) channel dot plots, as displayed in Figure 13, the unstained samples values were subtracted to those obtained for the stained ones.

3.5. Statistical analysis

Data statistics analysis were performed using GraphPad Prism™ 6.0 (GraphPad Software, USA). Comparisons were made using the two-way analysis of variance (ANOVA), followed by the Bonferroni's post-hoc test.

4. Results

4.1 Protocol optimization

4.1.1. Cellular density

The cellular density (cell counting) was determined by two distinct procedures: Neubauer chamber – concomitantly to the TB assay and FC. The results obtained for the tested samples (10 individuals = 28 samples: 10 VH-R, 10 VH-L and 8 CSF) during the optimization of the analytical protocol are summarized in Table 2.

Table 2 – Cellular density (U/mL) in the tested samples (VH-R, VH-L and CSF) as determined with NC and FC.

PMI (h)	Sample nº	Cellular density (U/mL)					
		NC			FC		
		VH-R	VH-L	CSF	VH-R	VH-L	CSF
14h45	**8**	5.00×10^4	1.08×10^6	1.13×10^6	4.16×10^4	2.08×10^6	1.25×10^7
14h55	**10**	1.50×10^5	4.20×10^5	1.02×10^6	2.40×10^4	6.76×10^5	1.25×10^7
26h25	**2**	7.15×10^5	2.40×10^5	NA	7.96×10^4	1.19×10^6	NA
32h20	**3**	8.00×10^4	4.50×10^4	5.95×10^5	1.25×10^7	8.33×10^6	2.50×10^7
34h55	**1**	1.38×10^4	2.75×10^4	1.68×10^5	4.24×10^5	4.63×10^4	4.39×10^5
35h05	**4**	4.75×10^5	1.80×10^5	4.00×10^5	3.01×10^4	5.10×10^5	3.16×10^5
60h10	**5**	3.45×10^5	2.20×10^5	NA	2.08×10^5	2.61×10^4	NA
62h00	**6**	6.40×10^5	1.00×10^5	5.60×10^6	1.47×10^6	2.32×10^4	7.58×10^5
63h00	**7**	1.35×10^5	2.35×10^5	2.86×10^6	3.22×10^4	6.10×10^5	2.50×10^7
69h55	**9**	9.50×10^4	4.30×10^5	2.25×10^5	1.64×10^5	3.57×10^6	1.25×10^6

NA – Not analyzed (due to contamination with red blood cells). CSF – Cerebrospinal fluid; FC – Flow cytometry; NC – Neubauer chamber; PMI – Postmortem interval; VH-L – Vitreous humor from left eyeball; VH-R – Vitreous humor from right eyeball.

Generally, it was observed that cellular density values (number of cells / unit volume) determined using the Neubauer chamber procedure were much lower than those obtained by FC for the same samples (Table 2). As shown in Figure 7, the difference was particularly noticeable for CSF.

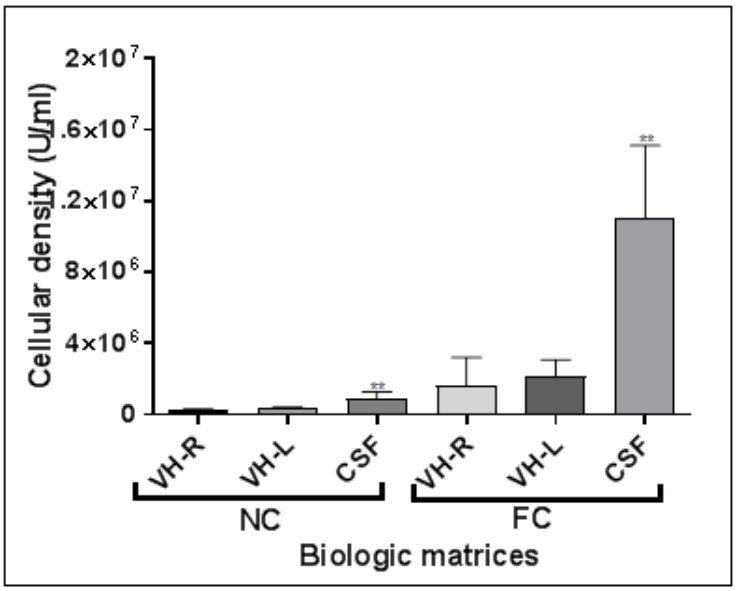

Figure 7 – Cellular density (U/mL) for VH-R, VH-L and CSF as determined by NC and FC procedures. CSF – Cerebrospinal fluid; FC – Flow cytometry; NC – Neubauer chamber; VH-L – Vitreous humor from left eyeball; VH-R – Vitreous humor from right eyeball; ** $p < 0.05$, comparing NC and FC methods for CSF cellular density. The values are given as the mean ± SEM (n = 10).

Table 2 data and Figure 7 also show that CSF presented a much higher cellular density than both VH-R and VH-L.

In what concerns the correlation with PMI, it was not possible to perceive a clear pattern of variation of cellular density over time. For NC data, it was observed a fluctuation of the results for VH-R from $5x10^4$ U/mL for PMI = 14h45, to $9,50x10^4$ U/mL for PMI = 69h55, with the maximum value of cellular density ($7,15x10^5$ U/mL) for PMI = 26h25; and for CSF from $1,13x10^6$ U/mL for PMI = 14h45 to $2,25x10^5$ U/mL for PMI = 69h55, with the maximum value of $5.60x10^6$ U/mL for PMI = 62 h. The same fluctuant behavior was observed for FC data for all matrices: in VH-R the values varied from $4,16x10^4$ U/mL for PMI = 14h45 to $1,64x10^5$ U/mL for PMI = 69h55, with the maximum value of $1,25x10^7$ U/mL for PMI = 32h20 h; in VH-L varied from $2,08x10^6$ U/mL for PMI = 14h45 to $3,57x10^6$ U/mL for PMI = 69h55, with the maximum of $8,33x10^6$ U/mL for PMI = 32h20; and in CSF varied from $1,25x10^7$ U/mL for PMI = 14h45 to $1,25x10^6$ U/mL for PMI = 69h55, with the maximum of $2,50x10^7$ U/mL for PMIs = 32h20 and 63 h.

4.1.2. Cellular viability

The results obtained for the cellular viability for all the tested samples during protocol optimization (n = 30 samples; 10 VH-R, 10 VH-L and 8 CSF) with both the TB assay (with NC cell counting) and FC are summarized in Table 3.

Table 3 – Cellular viability (%) for VH-R, VH-L and CSF as determined by TB assay and FC.

PMI (h)	Sample nº	Cellular viability (%)					
		TB			FC		
		VH-R	VH-L	CSF	VH-R	VH-L	CSF
14h45	8	0.00	31.16	82.22	0.00	31.16	82.22
14h55	10	13.33	0.00	89.71	13.33	0.00	89.71
26h25	2	5.59	37.50	NA	5.59	37.50	NA
32h20	3	37.50	100.00	41.18	37.50	100.00	41.18
34h55	1	52.92	67.86	51.40	52.92	67.86	51.40
35h05	4	48.42	16.67	23.75	48.42	16.67	23.75
60h10	5	15.94	6.82	NA	15.94	6.82	NA
62h00	6	13.28	15.00	87.67	13.28	15.00	87.67
63h00	7	62.96	40.43	91.26	62.96	40.43	91.26
69h55	9	10.53	46.51	80.00	10.53	46.51	80.00

NA – Not analyzed (due to contamination with red blood cells). CSF – Cerebrospinal fluid; FC – Flow cytometry; PMI – Postmortem interval; TB – Trypan blue assay (with Neubauer chamber cell counting); VH-L – Vitreous humor from left eyeball; VH-R – Vitreous humor from right eyeball.

Generally, it was observed that cellular viability values determined by the TB assay were quite similar to those obtained by FC (Table 3 and Fig. 8).

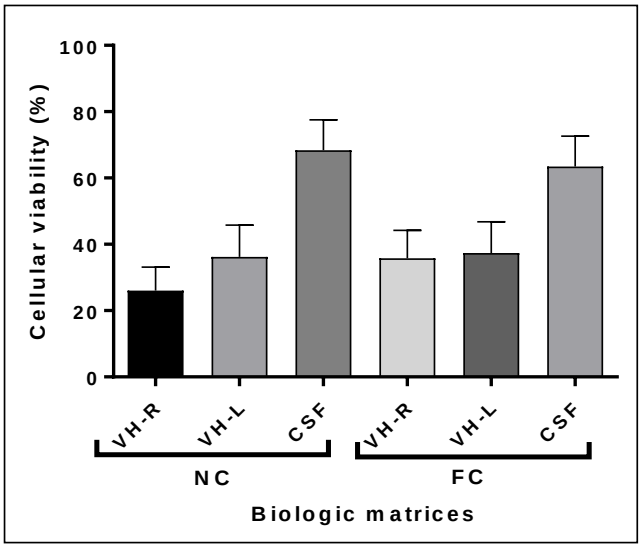

Figure 8 – Cellular viability (%) in VH-R, VH-L and CSF as determined by NC and FC procedures. CSF – Cerebrospinal fluid; FC – Flow cytometry; TB – Trypan blue assay ((with Neubauer chamber cell counting); VH-L – Vitreous humor from left eyeball; VH-R – Vitreous humor from right eyeball; ** $p < 0.05$, comparing NC and FC procedures for CSF cellular density. The values are given as the mean ± SEM (n = 10).

Table 3 and Figure 8 also clearly show that CSF presented higher levels of cellular viability than VH-R and VH-L, as evaluated by both NC-TP and FC procedures.

4.2 Samples analysis

After this initial study on methodological aspects, FC was selected to continue the work. Also, due to their low cell count, it was decided to mix the VH samples from left and right eyeballs of the same individual to increase the final sample volume. The work continued with the analysis of n=21 VH samples and n=17 CSF samples (4 CSF samples were excluded due to contamination with red blood cells), and the following parameters were studied: i) cellular density; ii) cells of interest and cellular debris; iii) cellular viability, and iv) apoptosis and necrosis. The results are presented below.

i) Cellular density

The cell counting values (U/mL) versus PMI for both VH and CSF samples are depicted in Figure 9. As observed, a poor correlation between variables was obtained, especially in VH samples.

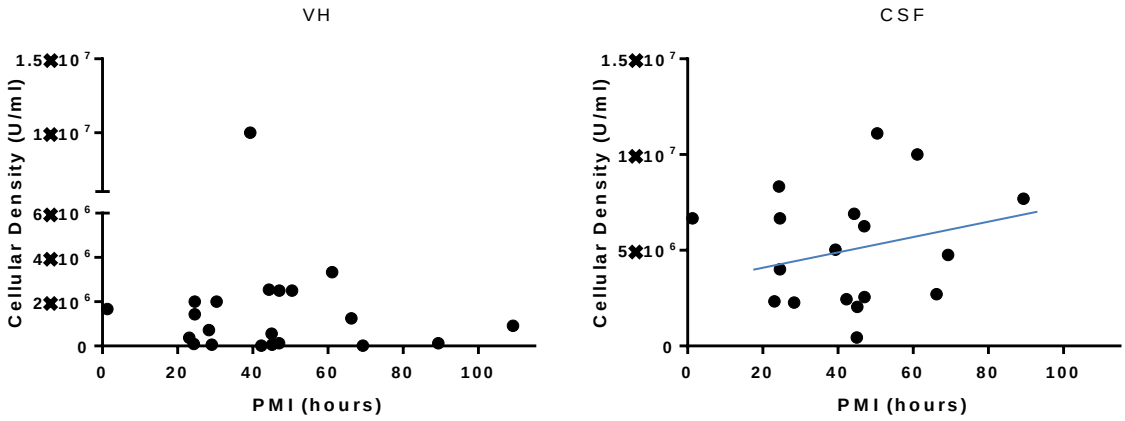

Figure 9 – Relationship between cellular density (U/mL) and PMI for both VH and CSF samples.

ii) Cells of interest and cellular debris

Representative dot plots of FC analysis of two samples [a) VH sample no. 24; b) CSF sample no. 20] are depicted in Figure 10.

The “cells of interest” and the “cellular debris” were defined, according to their size and complexity, through the polygon gates P1 and P2, respectively (drawn in red in the SSC vs. FSC dot plots shown in Figure 10).

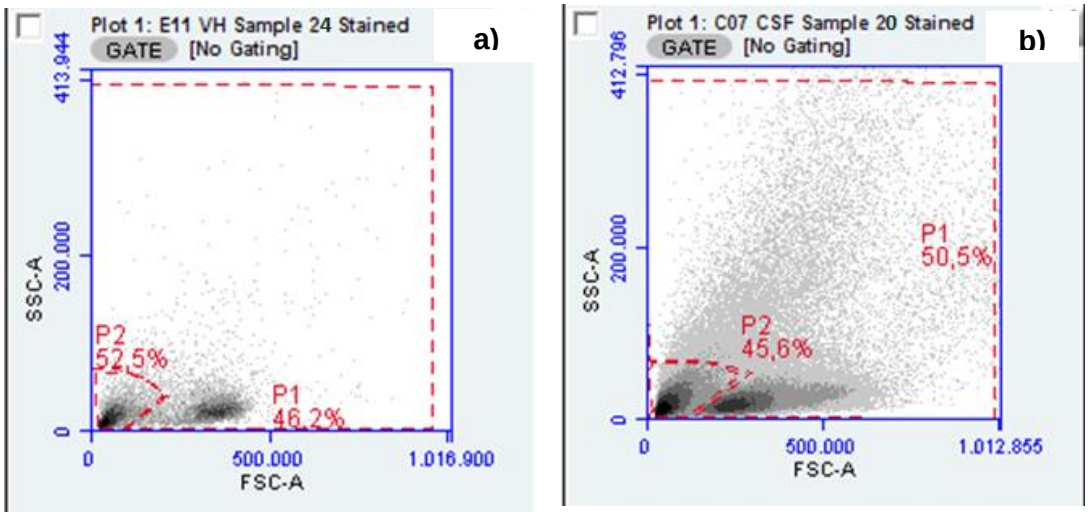

Figure 10 – Representative FC dot plots of SSC (Y-axis) and FSC (X-axis) parameters for a VH (a) and a CSF (b) samples.

For VH samples, the results obtained (P1 – cells of interest and P2 – cellular debris percentages) were related to the correspondent PMI as shown in Figure 11.

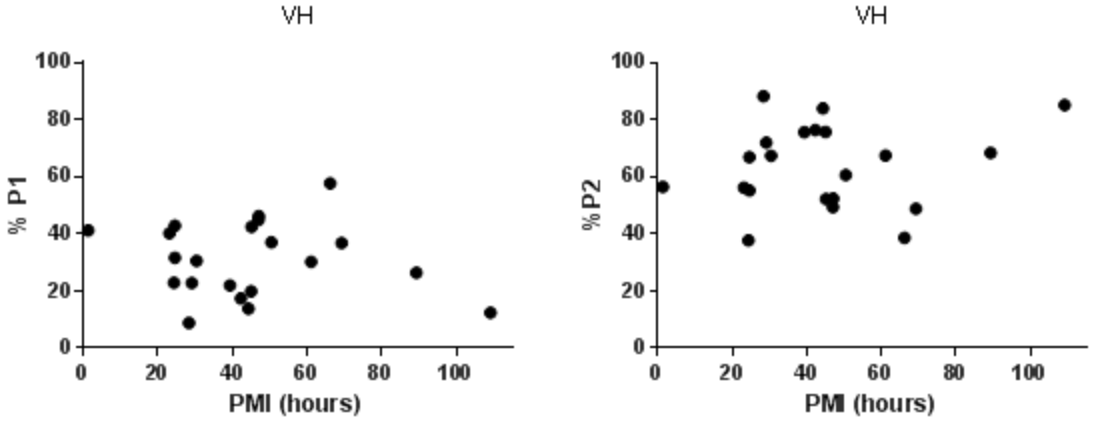

Figure 11 – Relationship between the parameter %P1 (cells of interest), %P2 (cellular debris) and PMI for VH samples.

The values of %P1 for VH samples (Figure 11, left) varied from a minimum of 8.87% for PMI = 28h35 to a maximum of 57.76% for PMI = 66h20.
The values of %P2 for VH samples (Figure 11, right) varied from a minimum of 37.76% at PMI = 24h31 to a maximum of 88.32% at PMI = 28h35.
The data showed a random scatter not dependent on PMI.

A similar graphic representation of the results obtained for CSF samples (P1 – cells of interest; P2 – cellular debris percentages) as a function of PMI is depicted in Figure 12.

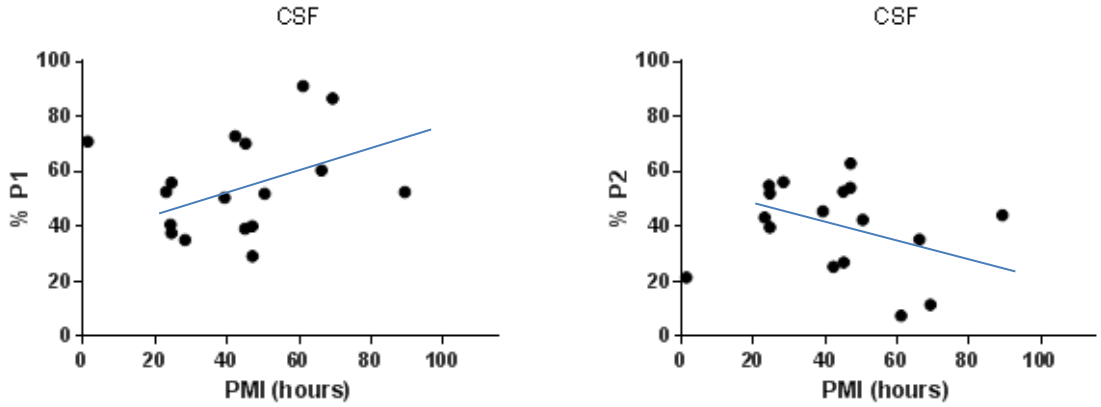

Figure 12 – Relationship between the parameter %P1 (cells of interest), %P2 (cellular debris) and PMI for CSF samples.

The most interesting finding is the quite similar data pattern between CSF and VH. Again, the %P1 values showed a clear tendency for increased cell levels with increased PMI (in the range 20-70 hours), and %P2 values showed an inverse relation with increased PMI (in the range 20-70 hours), in comparison with %P1. However, CSF samples presented a much higher %P1 (cells of interest) and lower %P2 (cellular debris) than VH.

iii) Cellular viability

The percentage of viable cells in CSF and VH samples was determined based on the percentage of events at quadrants Q1-LL or Q2-LL (lower left) in FL3 x FL1 dot plots (as displayed in Figure 14).

The relationship between the obtained data and PMI is shown on Figure 13.

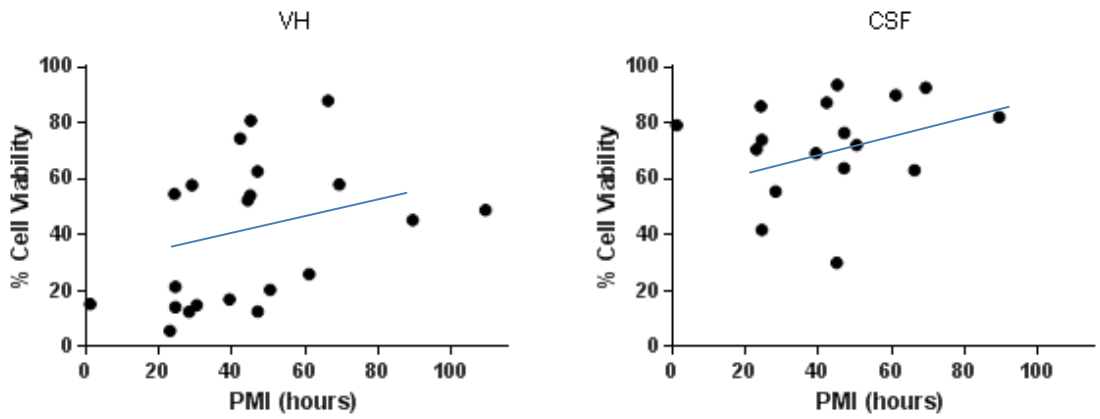

Figure 13 – Cellular viability (%) in VH and CSF samples as a function of PMI.

The percentage of viable cells in VH ranged from a minimum of 5.78% from PMI = 23h10 to a maximum of 88.04% for PMI = 66h20. The percentage of viable cells in CSF ranged from a minimum of 30.15% for PMI = 45h to a maximum of 93.71% for PMI = 45h15. Average cellular viability was much higher in CSF samples. In both cases, a tendency to increase between this parameter and PMI was observed.

iv) Apoptosis and Necrosis

As referred before, the percentage of apoptotic and necrotic cells was determined based on the percentage of events in the quadrant Q2-LR (lower right) for apoptosis; and on the percentage of events in the quadrant Q2-UR (upper right) for necrosis, of the FL3 (PI staining) x FL1 (A5–FITC) channel dot plots, as displayed in Figure 14.

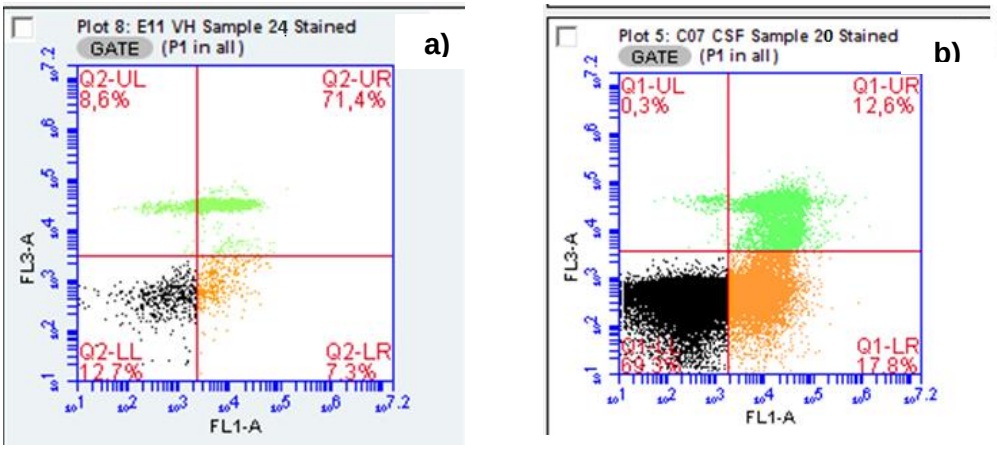

Figure 14 – Representative FC dot plots of FL3 (PI staining) and FL1 (A5–FITC staining) channel signal displaying the percentage of apoptosis (LR quadrants) and necrosis (UR quadrants) for both matrices: VH (a) and CSF (b).

a) Apoptosis

The percentage of apoptosis in VH (Figure 15, left) varied from a minimum of 7.10% for PMI = 47h04 to a maximum of 92.98% for PMI = 23h10. In CSF the percentage of apoptosis was somewhat lower (Figure 15, right). The percentage varied from a minimum of 3.91% for PMI = 47h04 to a maximum of 65.33% for PMI = 45h.

A tendency for increasing values with PMI was observed for VH samples but not for CSF, where the tendency was to decrease along PMI.

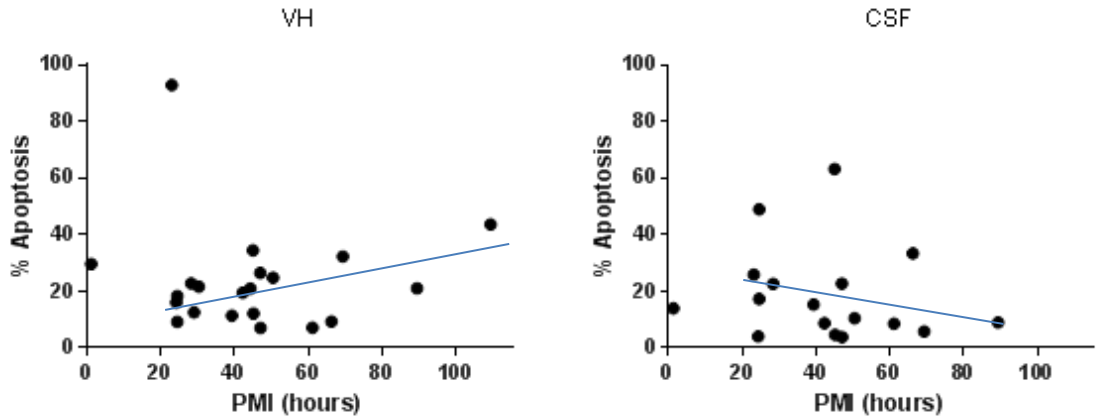

Figure 15 – Percentage of apoptotic cells in VH and CSF samples as a function of PMI.

b) Necrosis

The percentage of necrotic cells in VH and CSF samples are depicted in Figure 16. For VH (Figure 16, left) the values ranged from 0% for PMI = 23h10 to a maximum of 71.03% for PMI = 47h04. The highest values were found for PMI between 20-50 h, but no correlation with PMI was observed. In CSF (Figure 16, right) the percentage of necrosis was significantly lower (maximum of 14.38%), even at high PMI values (<15%), but an even random data scatter was observed.

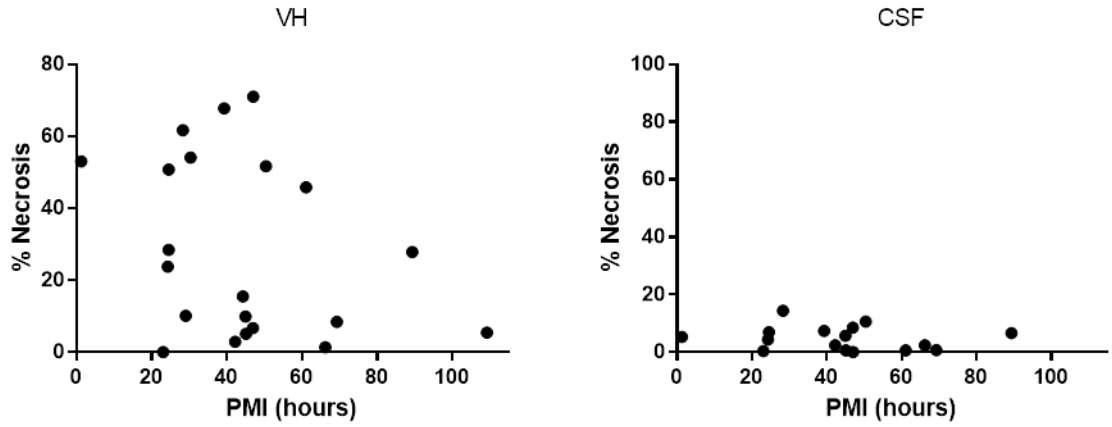

Figure 16 – Percentage of necrotic cells in VH and CSF samples as a function of PMI.

5. Discussion and Conclusions

In criminal investigation, PMI is an important parameter to be determined and a lot of studies have been performed to achieve this goal, such as biochemical studies of markers in bone marrow and other organs (which may be cells or proteins), immunohistochemical, with DNA/RNA, entomological and in bone remains, as reviewed by Hayman and Oxenham (2016). However, and according to our knowledge, no one has developed a sufficient accurate method to be used in daily forensic routine. Therefore, the pursuing to new methods and studies continues to be of paramount interest in this field.

Bardale (2009) performed a study with CSF to evaluate the alterations on the cells present in this matrix over time. The author concluded that the number of cells in this biological fluid increases over time after death and that up to 12 hours it was possible to identify the presence of different cell types, such as lymphocytes, neutrophils and monocytes, but after this period the identification / classification becomes very difficult. It should be noted that the samples used in the abovementioned work were collected by cisternal puncture, and from brain ventricles, and this may justify some differences regarding total cell counts.

In the present work two different biologic matrices, VH and CSF, collected from human corpses during autopsy procedures were studied. The main reasons to choose these matrices were: its anatomical location – more protected from decomposition than for e.g. blood samples and organs in general; no special sample pretreatment required; the different biochemical composition of each one (thus eventually allowing to obtain different information from each one); the fact that they are commonly used in other studies; and finally the fact they are easy to collect in medical autopsies.

The main objective of this study, as referred before, was to evaluate if PMI could be estimated through the analysis of cell death progression in the cells present in two biological matrices with different biochemical composition: VH and CSF. Different parameters were studied, such as cellular density and viability, apoptosis and necrosis. To achieve this goal, TB exclusion assay (with cell counting in Neubauer chamber under optical microscopy) and a FC approach using PI and A5–FITC staining were used.

TB exclusion test is an inexpensive method and does not require special equipment. It enables to obtain both quantitative and qualitative results and a quite convenient

evaluation of cell death progression that can help in the study of body's decomposition level. However, this procedure is time consuming and strongly depends on the investigator' knowledge and experience, making it subjective and poorly accurate.

On the contrary, FC requires specialized equipment to perform the analysis and it is faster to run the samples (it can count about 1000 to 10000 cells per second), thus being the technique of choice for the study of a large number of samples (Darzynkiewicz et al., 1997; Ferlini et al., 1997; Koopman et al., 1994; Schmid et al., 1994). Furthermore, for this specific study, one of the major advantages of FC is that through the analysis of a single sample it is possible to evaluate cellular density and viability, apoptosis and necrosis (instead of just cellular viability and unspecific death as in TB exclusion assay and cell counting under optical microscopy) and the simplicity of the procedure. However, FC has the disadvantage that it is not often possible to distinguish individual cells from cell aggregates.

Due to the advantages mentioned above, after the optimization step of the work, FC was elected to proceed the study.

For A5-FITC and PI binding assay, the individually collected VH-R and VH-L samples were mixed in a same plastic microtube in order to increase cell concentration and consequently a higher number of events in FC analysis. It is important to note that during the optimization of the procedure no statistically significant difference ($p > 0.05$) was observed between the results obtained for cellular density and viability in the two eyeballs samples, nor for TB exclusion assay neither for FC analysis (cf. Table 2 and Figure 6).

Generally, CSF presented much higher cellular counts than both VH-R and VH-L. Therefore, CSF seems to be a much more appropriate biological matrix for this kind of studies.

As referred above, the main study (n=21 samples of VH and n=17 samples of CSF) was conducted using only FC. A flow cytometric approach using PI and A5–FITC staining was used.

Regarding cellular density it seems to exist a tendency to increased values with PMI observed for CSF, which is in accordance with a previous study from Bardale (2009).

Regarding “cells of interest” (P1) and “cellular debris” (P2), no conclusions can be drawn. An inverse relationship was expected between these parameters because they are complementary. For VH samples there was no direct relationship with PMI neither for P1 nor for P2, but P2 percentages were much higher than P1 in this matrix. For CSF samples (Figure 12), an inverse relationship between “cells of interest” (P1) and “cellular debris” (P2) was observed. P1 tended to increase with PMI, and according to Bardale (2009), this may be due to the migration of cells to CSF during the first hours after death.

The % of cellular viability in VH seemed to increase but in two parallel lines, reflecting a great inter-individual variability. Therefore a common model cannot be assumed. For CSF this tendency to increased values with PMI was also observed, with a higher correlation coefficient (Figure 13).

The parameter % apoptosis showed a conflicting tendency (to decrease with PMI in CSF and to increase in VH). The % necrosis showed no tendency for both matrices. The data were random scatter with no relationship to PMI.

In summary, this study showed that the flow cytometric approach used (involving PI and A5–FITC staining) has potential to generate important information regarding cellular changes after death. However, no direct correlation was found between any of the parameters tested (related to progression of cell death) and PMI.

The present work has as major limitation which is the absence of an exact knowledge of the PMI of each individual studied (because of the absence of exact information about the time at which the dead occurred). So, this study needs to be continued in order to increase the number of analyzed individuals and to extend the range of PMI studied.

In future works it is important to consider the possibility of study individuals who died at hospitals, in controlled environmental conditions which would allow more accurate time of dead determination.
Looking to the literature, this study was pioneer in using FC analysis to evaluate the progression of cell death overtime in VH and CSF in order to use this approach in the future to estimate PMI.

6. References

Angi M, Kalirai H, Coupland SE, Damato BE, Semeraro F and Romano MR (2012) Proteomic Analyses of the Vitreous Humour. *Mediators of Inflammation* **2012**:7.

Ansari N, Müller S, Stelzer E and Pampaloni F (2013) *Quantitative 3D Cell-Based Assay Performed with Cellular Spheroids and Fluorescence Microscopy*.

Arends MJ, Morris RG and Wyllie AH (1990) Apoptosis. The role of the endonuclease. *The American Journal of Pathology* **136**:593-608.

Bardale R (2009) Evaluation of cerebrospinal fluid cells in postmortem period to estimate death interval. *J Indian Acad Forensic Med* **31**:3.

Bate-Smith EC and Bendall JR (1947) Rigor mortis and adenosine-triphosphate. *The Journal of Physiology* **106**:177-185.

Beran RG (2010) What is legal medicine--are legal and forensic medicine the same? *Journal of forensic and legal medicine* **17**:137-139.

Bévalot F, Cartiser N, Bottinelli C, Fanton L and Guitton J (2016) Vitreous humor analysis for the detection of xenobiotics in forensic toxicology: a review. *Forensic Toxicology* **34**:12-40.

Brown M and Wittwer C (2000) Flow cytometry: principles and clinical applications in hematology. *Clinical chemistry* **46**:1221-1229.

Clark M, Worrell M and Pless J (1997) Postmortem Changes in Soft Tissues, in *Forensic Taphonomy: The Post-mortem Fate of Human Remains* (Haglund WD, Sorg, M.H. ed) pp 151-164, CRC Press.

Damkier HH, Brown PD and Praetorius J (2013) Cerebrospinal Fluid Secretion by the Choroid Plexus. *Physiological Reviews* **93**:1847-1892.

Darzynkiewicz Z, Juan G, Li X, Gorczyca W, Murakami T and Traganos F (1997) Cytometry in cell necrobiology: analysis of apoptosis and accidental cell death (necrosis). *Cytometry* **27**:1-20.

Escobar-Sánchez ML, Sánchez-Sánchez L and Sandoval-Ramírez J (2015) Steroidal Saponins and Cell Death in Cancer, in *Cell Death - Autophagy, Apoptosis and Necrosis* (Ntuli TM ed) p Ch. 15, InTech, Rijeka.

Ferlini C, Kunkl A, Scambia G and Fattorossi A (1997) The use of Apostain in identifying early apoptosis. *Journal of immunological methods* **205**:95-101.

Fink SL and Cookson BT (2005) Apoptosis, pyroptosis, and necrosis: mechanistic description of dead and dying eukaryotic cells. *Infection and immunity* **73**:1907-1916.

Forbes SL (2008) Decomposition Chemistry in a Burial Environment, in *Soil Analysis in Forensic Taphonomy* pp 203–223.

Gill-King H (1997) Chemical and Ultrastructural Aspects of Decomposition, in *Forensic Taphonomy: The Postmortem Fate of Human Remains* (Haglund WD and Sorg MH eds) pp 93-108, CRC Press.

Green DR (2017) Cell death and the immune system: getting to how and why. *Immunological Reviews* **277**:4-8.

Hayman J and Oxenham M (2016) *Human Body Decomposition*, Academic Press, Australia.

Hingorani R, Deng J, Elia J, McIntyre C and Mittar D (2011) *Detection of apoptosis using the BD annexin V FITC assay on the BD FACSVerse™ system*.

Johanson C, Stopa E, Baird A and Sharma H (2011) Traumatic brain injury and recovery mechanisms: peptide modulation of periventricular neurogenic regions by the choroid plexus-CSF nexus. *Journal of neural transmission (Vienna, Austria : 1996)* **118**:115-133.

Kerr JF, Wyllie AH and Currie AR (1972) Apoptosis: a basic biological phenomenon with wide-ranging implications in tissue kinetics. *British Journal of Cancer* **26**:239-257.

Kobayashi M, Ikegaya H, Takase I, Hatanaka K, Sakurada K and Iwase H (2001) Development of rigor mortis is not affected by muscle volume. *Forensic science international* **117**:213-219.
Koopman G, Reutelingsperger CP, Kuijten GA, Keehnen RM, Pals ST and van Oers MH (1994) Annexin V for flow cytometric detection of phosphatidylserine expression on B cells undergoing apoptosis. *Blood* **84**:1415-1420.
Krompecher T (1981) Experimental evaluation of rigor mortis V. Effect of various temperatures on the evolution of rigor mortis. *Forensic science international* **17**:19-26.
Lee Goff M (2009) Early post-mortem changes and stages of decomposition in exposed cadavers. *Experimental & applied acarology* **49**:21-36.
Madea B and Kernbach-Wighton G (2013) Early and Late Postmortem Changes A2 - Siegel, Jay A, in *Encyclopedia of Forensic Sciences* (Saukko PJ and Houck MM eds) pp 217-228, Academic Press, Waltham.
Mathur A and Agrawal YK (2011) An overview of methods used for estimation of time since death. *Australian Journal of Forensic Sciences* **43**:275-285.
Perper JA (2006) Time of death and changes after death. *Spitz and Fisher's Medico Legal Investigation of Death*:107-108.
Prieto J, Magana C and Ubelaker D (2004) Interpretation of Postmortem Change in Cadavers in Spain.
Puntis M, Reddy U and Hirsch N (2016) Cerebrospinal fluid and its physiology. *Anaesthesia & Intensive Care Medicine* **17**:611-612.
Purves D, Fitzpatrick D, Katz LC, Lamantia AS, McNamara JO, Williams SM and Augustine GJ (2001) *Neuroscience*, Sinauer Associates.
Remington LA (2011) *Clinical Anatomy of the Visual System E-Book*, Elsevier Health Sciences.
Sachdeva N, Rani Y, Singh R and Murari A (2011) Estimation of Post-Mortem Interval from the Changes in Vitreous Biochemistry. *J Indian Acad Forensic Med* **33**:171-174.
Saukko P and Knigth B (2004) *Forensic Pathology*, Edward Arnold, London.
Schmid I, Uittenbogaart CH, Keld B and Giorgi JV (1994) A rapid method for measuring apoptosis and dual-color immunofluorescence by single laser flow cytometry. *Journal of immunological methods* **170**:145-157.
Spector R, Robert Snodgrass S and Johanson CE (2015) A balanced view of the cerebrospinal fluid composition and functions: Focus on adult humans. *Experimental Neurology* **273**:57-68.
Stoddart MJ (2011) Cell viability assays: introduction. *Methods in molecular biology (Clifton, NJ)* **740**:1-6.
Stratchko L, Filatova I, Agarwal A and Kanekar S (2016) The Ventricular System of the Brain: Anatomy and Normal Variations. *Seminars in ultrasound, CT, and MR* **37**:72-83.
Strober W (2001) Trypan blue exclusion test of cell viability. *Current protocols in immunology*.
Tenreiro MM, Ferreira R, Bernardino L and Brito MA (2016) Cellular response of the blood-brain barrier to injury: Potential biomarkers and therapeutic targets for brain regeneration. *Neurobiology of Disease* **91**:262-273.
Ubelaker DH and Zarenko KM (2011) Adipocere: What is known after over two centuries of research. *Forensic science international* **208**:167-172.
Vanezis P and Trujillo O (1996) Evaluation of hypostasis using a colorimeter measuring system and its application to assessment of the post-mortem interval (time of death). *Forensic science international* **78**:19-28.
Vermes I, Haanen C and Reutelingsperger C (2000) Flow cytometry of apoptotic cell death. *Journal of immunological methods* **243**:167-190.
Wlodkowic D, Telford W, Skommer J and Darzynkiewicz Z (2011) Apoptosis and Beyond: Cytometry in Studies of Programmed Cell Death. *Methods in Cell Biology* **103**:55-98.

Appendixes

Appendix 1 – Responsibility term assigned to ask collaboration of INMLCF of Porto.

REPÚBLICA PORTUGUESA

TERMO DE RESPONSABILIDADE

Mónica Cristina Francisco Tomé, portador(a) do Cartão de Cidadão/Bilhete de Identidade n.º 14032802, válido até 4/09/2017, tendo requerido autorização para realizar um estágio e/ou para realizar um estudo de investigação no Serviço/Gabinete Médico-Legal e Forense da Delegação do Norte do Instituto Nacional de Medicina Legal e Ciências Forenses, I.P. (INMLCF), desde já declara:

- Que cumprirá todas as instruções e indicações que lhe forem dadas em matéria de funcionamento do Serviço;
- Que aceita e cumprirá as restrições, os termos e as condições que lhe forem colocados no acesso à informação;
- Que não vai apossar-se de material iconográfico, de cópia de relatórios ou de outro tipo de elementos, ou de qualquer base de dados;
- Que não procederá ao registo de qualquer elemento identificativo dos processos, designadamente elementos de identificação do examinado e número do processo judicial e respetivo Tribunal, e manterá completo sigilo sobre qualquer informação de serviço e sobre qualquer facto de natureza pericial a que eventualmente possa aceder;
- Que entregará cópia digital e em papel da(s) publicação(ões) efetuadas;
- Que obrigatoriamente referirá a fonte INMLCF, I.P., em quadros, tabelas ou imagens, independentemente da modalidade da apresentação dos dados.

Mais declara que a violação de qualquer dos compromissos aqui assumidos resultará no apuramento de responsabilidades penais, civis, e disciplinares, e ainda à impossibilidade, imediata e futura, de o INMLCF, I.P. lhe conceder qualquer tipo de colaboração.

6/10/2016

O(A) Declarante

Mónica Cristina Francisco Tomé

Página 1 de 2

Appendix 2 – Authorization of INMLCF of Porto to collaborate in the study.

REPÚBLICA PORTUGUESA

Exma. Senhora Diretora do Departamento de Investigação, Formação e Documentação
Instituto Nacional de Medicina Legal e Ciências Forenses, I.P.

ASSUNTO

Requerente: Mónica C. F. Tomé. Pedido de recolha de amostras em cadáver para utilização nas instalações da Faculdade de Farmácia - UP no âmbito de Mestrado em Ciências Forenses da FMUP.

DESPACHO

Relativamente ao assunto em epígrafe, não obstante a documentação recebida pelo RAI incluir já a autorização do pedido, dada pelos responsáveis do competente serviço técnico da Delegação do Norte do INMLCF, e pela Diretora desta, impõe dizer-se:

Nos termos das disposições conjugadas dos artigos 2º, 3º, e 5º, é admissível a recolha e utilização das amostras para os fins de investigação científica pretendidos, desde que observados os requisitos aí referidos, designadamente a consulta da RENNDA, e o integral respeito pela finalidade de utilização pretendida. Deve cumprir-se ainda o disposto nos artigos 7º, 8º e 18º da mencionada Lei (quanto à conservação, documentação e destino das amostras). O acesso da requerente aos cadáveres deve garantir o sigilo e a confidencialidade da informação pessoal. Respeitante a cada caso, e a recolha das amostras não pode prejudicar minimamente a realização e a finalidade da autópsia médico-legal.

8 de março de 2017

O Responsável pelo Acesso à Informação

Diogo Pinto da Costa